



HAL
open science

Steady photo-darkening of thulium alumino-silicate fibers pumped at 1.07 μm : Quantitative effect of lanthanum, cerium and thulium.

Jean-François Lupi, Manuel Vermillac, Wilfried Blanc, Franck Mady, Mourad Benabdesselam, Bernard Dussardier, Daniel R. Neuville

► To cite this version:

Jean-François Lupi, Manuel Vermillac, Wilfried Blanc, Franck Mady, Mourad Benabdesselam, et al.. Steady photo-darkening of thulium alumino-silicate fibers pumped at 1.07 μm : Quantitative effect of lanthanum, cerium and thulium.. Optics Letters, 2016. hal-01340389

HAL Id: hal-01340389

<https://hal.science/hal-01340389>

Submitted on 1 Jul 2016

HAL is a multi-disciplinary open access archive for the deposit and dissemination of scientific research documents, whether they are published or not. The documents may come from teaching and research institutions in France or abroad, or from public or private research centers.

L'archive ouverte pluridisciplinaire **HAL**, est destinée au dépôt et à la diffusion de documents scientifiques de niveau recherche, publiés ou non, émanant des établissements d'enseignement et de recherche français ou étrangers, des laboratoires publics ou privés.



Distributed under a Creative Commons Attribution - NonCommercial 4.0 International License

Steady photo-darkening of thulium aluminosilicate fibers pumped at 1.07 μm : Quantitative effect of lanthanum, cerium and thulium.

Jean-Francois Lupi¹, Manuel Vermillac¹, Wilfried Blanc^{1,*}, Franck Mady¹, Mourad Benabdesselam¹, Bernard Dussardier¹, and Daniel R. Neuville²

¹Universit Nice Sophia Antipolis, CNRS, Laboratoire de Physique de la Matire Condense, UMR7336, Parc Valrose 06108 Nice, France

²Équipe des gomatriaux, IGP, COMUE Sorbonne Paris-Cit, CNRS UMR 7154, 1 rue Jussieu, 75005 Paris, France

July 1, 2016

Abstract

By pumping thulium-doped silica-based fibers at **1.07 μm** , rapid generation of absorbing centers leads to photo-induced attenuation (PIA). This detrimental effect prevents exploiting laser emissions in the visible and near infrared. We report on the characterization of the PIA versus the fiber core composition, particularly the concentration of thulium (***Tm***), lanthanum (***La***) and cerium (***Ce***) ions. We show that UV emission induced by ***Tm-Tm*** energy transfers is the source of photo-darkening, and that lanthanum and cerium are efficient hardeners against PIA.

Silica as a glass host for rare-earth (RE) doped lasers and amplifiers offers the best performances in terms of efficiency, power, reliability and cost effectiveness [1]. It is indeed chemically stable, mechanically robust and its optical transparency is high in the visible and the near-infrared (NIR) range up to 2 μm . Some new applications of RE-doped silica materials require to develop optical transitions at wavelengths shorter than 0.85 μm [2]. Applications of RE-transitions in the visible, or in uncovered spectral ranges in the NIR, are possible when using so called soft glasses, that are transparent in these ranges. In particular, glasses based on zirconium fluoride, like ZBLAN, have allowed many demonstrations of lasers and amplifiers from 0.45 to 3.9 μm [3]. These glasses have a lower phonon-energy than silica: this allows high population inversion and efficient up-conversion pumping schemes. However, compared to silica, soft glasses are chemically and mechanically less stable, and are more expensive. Further, their threshold to optical damage is too low for the development of high power fiber applications.

Among the RE ions, thulium (Tm^{3+}) is particularly interesting because it offers many potential optical transitions spanning from 0.45 to 1.9 μm . Except for the current pumping scheme at 0.79 μm which provides efficient amplification around 1.9 μm through a down-conversion energy transfer process [4], none of the other transitions are exploited in silica. An interesting up-conversion pumping scheme using a pump source at 1.07 μm provides up to seven laser emissions (spanning from 0.45 to 1.9 μm) that were implemented in ZBLAN fibers [3]. If one applies this scheme on a *Tm*-doped silica fiber, two phenomena will hamper amplification: fluorescence quenching by non-radiative decay and transparency degradation by photo-darkening [5]. The high phonon-energy of sil-

ica glass (as compared with fluorides) induces fast non-radiative decays from most energy levels of thulium, causing a strong reduction of their effective lifetime and hence the reachable population inversion, even under strong pumping. In *Tm*-doped silica, the non-radiative decays from the 3H_4 excited level may be mitigated by highly co-doping with aluminum, promoting the amplification of the 0.8 and 1.47 μm emission bands as well as up-conversion to higher energy levels (see Figure 1) [6–8]. Because the sought applications necessitate high concentrations of aluminum and thulium, strong photodarkening is observed [5, 9]. Besides, pumping of RE-doped optical fibers may cause the degradation of the transparency of both silica and fluoride glasses, especially when they are heavily doped [5, 9–13]. In the case of thulium-doped silica fiber pumped at 1.07 μm , photo-darkening (or photo-induced attenuation, PIA) is particularly fast and intense, enough to prevent amplification in the extended-visible region (0.45–0.9 μm) [5]. The aim of this paper is to quantify the effects of the concentrations of *Tm*, *La* and *Ce* on the photo-darkening mechanism. The positive effects of reduction of photo-darkening have been already reported for ytterbium-doped fibers by co-doping with *Ce* and explained by the ability of *Ce* to exist both in 3+ and 4+ valence states [10, 14]. *La* is of interest in this study because it exists only in one valence state (3+) and is optically inactive (no absorption band). Here we show that the co-doping of *Tm*-doped silica fibers with either cerium or lanthanum causes a reduction of the PIA under 1.07 μm pumping. We propose a systematic study on the effect of *Tm* and codopant concentrations on the PIA.

Fibers samples were prepared in our laboratory, using MCVD, solution doping and a drawing tower. The concentrations of *Al*, *Tm*, *La* and *Ce* were measured by elec-

tron probe micro analysis (EPMA) in the fibers. Three sets of samples were prepared. In each set, the concentration of only one ion varies (Table 1). Attenuation spectra were measured using the cut back method on all samples. Taking the mode/dopant overlap factor into account for each fiber sample (typically 0.6 to 0.8), a linear correlation is obtained between attenuation values measured at 1190 nm (hump on the 3H_5 level ground state absorption band) and EPMA concentration, leading to a correspondence of 1 dB/m at 1190 nm for ~ 18 ppm.at of Tm^{3+} .

Table 1: Concentrations (ppm.at of all elements incl. oxygen)

Series	Tm	La	Ce	Al
Tm	0-600	-	-	~ 8000
La	190 ± 30	0-7000	-	~ 8000
Ce	260 ± 40	-	0-1300	~ 8000

Figure 1 describes the experimental setup used to measure the PIA. The pump laser at 1.07 μm is a continuous wave ytterbium-doped fiber laser. It is coupled into a commercial passive fiber (Corning, HI-1060) through a telescope, a high reflection dielectric mirror, a dichroic mirror and an aspherical lens. The dichroic mirror is highly reflective at 1.07 μm and transparent from 0.55 to 1.0 μm . The input fiber end is cleaved at right angle. The fiber under test (FUT) samples are spliced to the input fiber. The typical length of samples is about 2 cm, short enough to neglect the pump depletion. Another passive HI-1060 fiber is spliced at the other end of FUT. A super continuum source (SCS) is coupled into the passive fiber in the counter-propagative direction relative to the pump beam, using two metallic mirrors (not represented) and an aspherical lens. The remaining pump is rejected by a second dichroic mirror, so that the SCS is protected against laser damage. The infra-red part of the SCS ($\lambda > 1$ m) is filtered out by a short-pass filter before the coupling into the fiber. When necessary, two band pass filters are placed before and after the FUT. The bandwidth of band pass filters is 2 nm at the central wavelength 550 nm. Their extinction ratio is higher than 40 dB. Next, the green 2 nm broad beam is called the probe.

The injected pump is measured by a power meter before the splicing of the FUT. Spectrally and time resolved measurements of the PIA were performed. The PIA spectra were measured from 550 to 1000 nm, at room temperature. To this aim, the band pass filters were removed and the OSA (Anritsu, MS9030A, 350-1750 nm) was used. A reference spectrum is recorded before the pump is turned on, and a second one is recorded just after the pump is turned off. In this configuration, the power of the SCS beam coupled into the FUT is typically less than 1 mW. To minimize the photo-bleaching which may be induced by the probe, the SCS is turned off during pump exposure. Just after the pump laser is turned off, the OSA is set to record the spectrum within 10 seconds only. The PIA spectrum (in dB/m) is computed from transmission spectra and normalized by the FUT length (~ 2 cm). The time-resolved PIA measurement was recorded at 550 nm while pumping at 1070 nm. This probe wavelength was

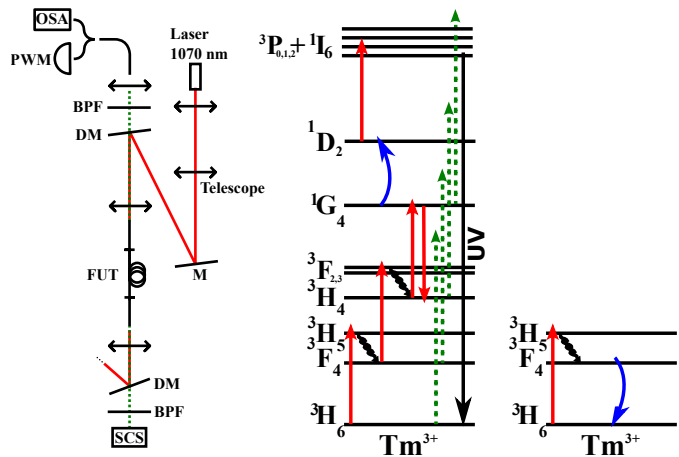


Figure 1: (Left): Experimental setup for PIA measurement. M: dielectric mirror, FUT: fiber under test, BPF: band pass filter, DM: dichroic mirror, OSA: optical spectrum analyzer, SCS: supercontinuum source, PWM: power meter. (Right): Energy level diagram of Tm^{3+} : red: pump induced transitions, blue: energy transfer, green: 550 nm probe.

selected because the PIA is strong whereas there is no absorption band of Tm ions at 550 nm. The band pass filters are placed, the SCS is turned on, and the PWM (Si photo-diode) is used to continuously measure the transmitted probe while pumping. The recording is continued after the laser is turned off, in order to check that almost no bleaching is caused by the probe.

Figure 2 shows the PIA spectra obtained by measuring of the power of the transmitted SCS beam before and after laser exposure at 750 mW during 30 minutes, for representative samples studied in this work: La 1800 ppm.at, Ce 300 ppm.at and Tm 160 ppm.at.

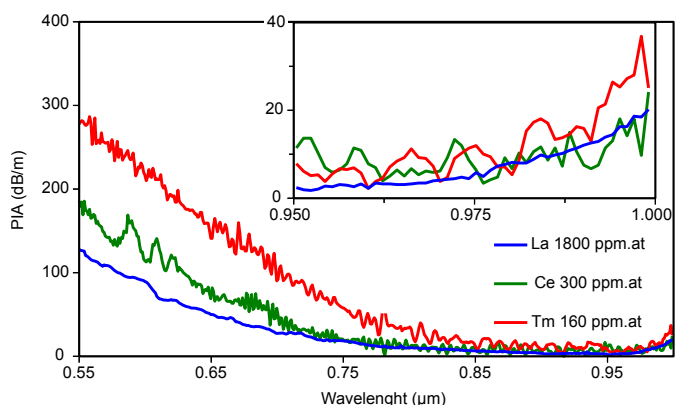


Figure 2: PIA spectra from selected samples after 1.07 μm laser exposure for 30 min (pump power 750 mW). The resolution is 10 nm for the La samples and 1 nm for the Ce and Tm samples. Acquisition time is 10 seconds. Inset: Zoom on the near infra-red region.

By pumping the fiber at 1.07 μm , two absorption (PIA) appear, a broad and strong absorption in the visible ($\lambda < 900$ nm) and a weak one in the near infra-red ($\lambda > 950$ nm)

(Figure 2). The latter band is not fully scanned because of the dichroic mirrors cut-off above 1000 nm. Cerium ions (both 3+ and 4+) absorb at wavelengths shorter than 400 nm [15–19] and *La* is optically inactive. Hence, these two absorptions cannot be attributed to direct absorptions by *La* or *Ce*. Therefore, PIA absorption are mainly related to the presence of both *Tm* and *Al* ions. The visible band has been already reported in rare-earth doped alumina-silica fiber and it is related to the presence of *Al* induced absorbing centers [11]. On the contrary, the infra-red absorption band has not been reported in non thulium-doped alumina silicates [11, 20], indicating that it could be related to *Tm* ions. An absorption band in near infra-red has been reported in CaF_2 and was attributed to 4f-4f transitions of Tm^{2+} [21]. This suggests that during the photo-darkening process, charge transfers would generate color centers, as in *Yb*-doped fibers, and in addition would reduce Tm^{3+} into Tm^{2+} , as already observed with *Er* ions [20]. 4f-5d absorption bands of Tm^{2+} are also expected and may also contribute to the visible band [21].

Figure 3 shows the steady PIA (PIAst) versus the thulium concentration for the *Tm* series. The inset shows the temporal curves. The PIA converges to a steady state (PIAst) as described in [13]. The PIAst value for the *Tm* series increases from 0 to 1300 dB/m when the thulium concentration increases from 0 to 600 ppm.at. The best candidate as a function to fit the results is a power-law, with an exponent equals to $\frac{1}{2}$ for the dependence on *Tm* concentration (solid line in Figure 3). The same trend was observed in *Yb*-doped silica with varying *Tm* concentration and probe light at 633 nm [9].

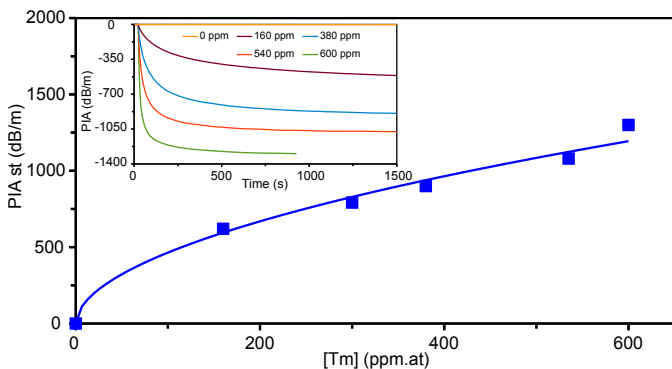


Figure 3: Steady state PIA (PIAst) versus thulium concentration in the Al-Tm-codoped *Tm* series, recorded at 550 nm. Pump power: 1 W. Squares: experimental data, solid line: power-law fit with exponent = $\frac{1}{2}$. Inset: corresponding temporal curves.

PIAst was measured in both *La* and *Ce* series. Its behaviour versus the concentration of lanthanum in the *La* series is shown in Figure 4. The point at 0 ppm.at *La* is extracted from Figure 3. When *La* concentration increases up to 4000 ppm.at, the PIAst reduces from 675 to less than 300 dB/m. Above 4000 ppm.at PIAst is almost constant.

The PIAst versus the concentration of cerium in the *Ce* series is shown in Figure 4. Cerium reduces the PIAst from 795 to 44 dB/m when the *Ce* concentration varies

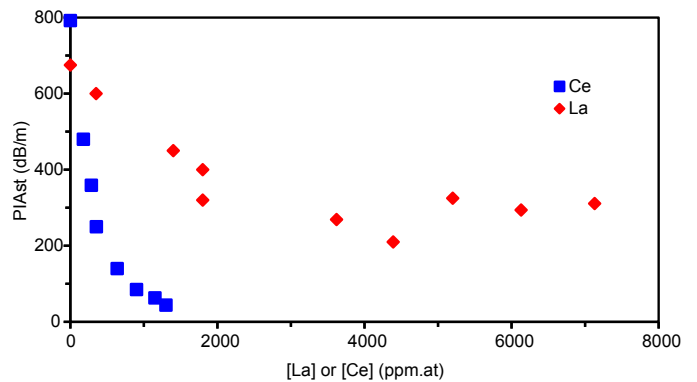


Figure 4: Steady state PIA (PIAst) versus cerium concentration in the *Ce* (Ce-Al-Tm) series (Blue) and versus lanthanum concentration in the *La* (La-Al-Tm) series (Red), recorded at 550 nm. Pump power: 1 W. Squares: experimental data.

from 0 to 1300 ppm.at.

Based on these results, we propose the following interpretation. Clusters of rare-earth, defects in glass matrix and generation of UV photons by energy transfers are usually invoked as the cause of photo-darkening [11]. Such mechanisms may be identified to explain the behaviour of PIAst when the *Tm* content increases. It is well known that when the *Tm* concentration increases, clusters tend to form, even with aluminum co-doping [22, 23]. By pumping the fiber at 1.07 μm , Tm^{3+} is excited up to the 1G_4 level (Figure 5). Then, the *Tm*-clusters promotes the energy transfer between *Tm* ions to populate the 1D_2 level. The population of this level is characterized by emissions bands at 520, 540, 660 and 740 nm (not shown). Thanks to the absorption of a fifth 1.07 μm photon, higher levels are reached ($^1I_6, ^3P_{0,1,2}$) (Figures 1 and 5), leading to emission of UV photon [24]. This UV photon can ionize defects in alumino-silicates (e.g. AlOHC, Al-Er, NBOHC, ODC [25]), leading to the promotion of an electron in the conduction band. This electron may recombine on a Tm^{3+} ion to form a Tm^{2+} ion or be trapped by a precursor center and form a color center. These steps are related to the formation of PIA. Steady state is reached because Tm^{2+} ions and “Defect 2” can be ionized by absorbing two pump photons (Figure 5). All these steps are depicted in an animated sequence available as supplementary material (see Visualization 1).

As La^{3+} ion is optically inactive, the main influence of this ion should be related to structural effects. When the RE ion is added into alumino-silicate glasses, it acts as a charge compensator if $\frac{[Al_2O_3]}{[RE_2O_3]} \leq 3$ [26]. As a consequence, RE is located preferentially close to the tetra-coordinated Al^{IV} species [26]. *La* and *Tm* compete to be located close to Al^{IV} species. Therefore, *La* tends to reduce the probability of *Tm*-cluster formation and hence the emission of UV photons. The same role for *La* has been proposed in erbium-lanthanum-doped silica fibers [27]. For *La* concentration above 4000 ppm.at, the influence of *La* changes. As *Al* content is about 8000 ppm.at, these concentrations of *La* are above the

threshold requested for the charge compensation (typically 2500 *ppm.at La* in our case). Then, *La* acts as network modifier and depolymerize the silica network. This depolymerization may lead to the formation of new color-centers which may absorb in the visible as already observed with Ce^{3+} ions [28]. A change of Tm^{3+} ions environment is also possible. For example, a higher content of *La* in the *Tm* environment may decrease the local phonon energy ($E_p(La_2O_3) = 400cm^{-1}$, $E_p(Al_2O_3) = 870cm^{-1}$, $E_p(SiO_2) = 1100cm^{-1}$), then enhance the population in 1G_4 level, and therefore the energy transfer mechanism [6–8].

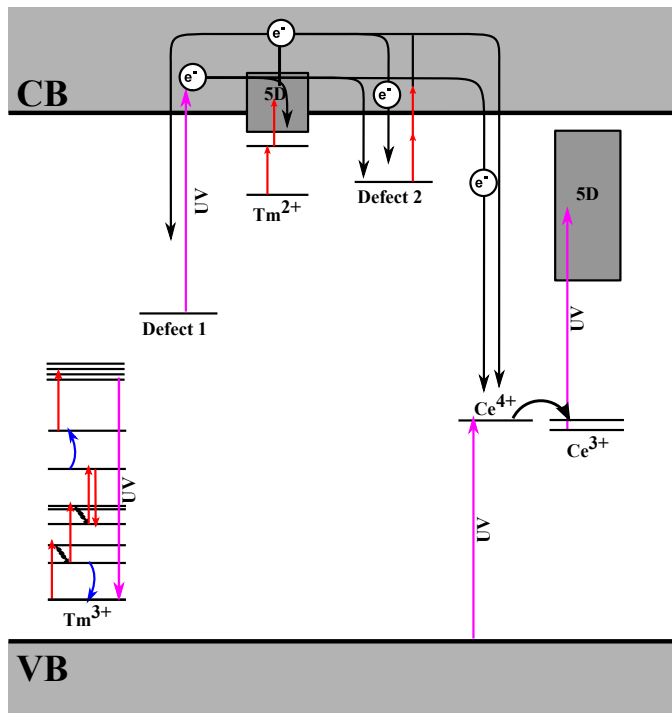


Figure 5: Schematic representation of photo-darkening process, for *Tm* pumped at 1.07 μm . An animated sequence of these mechanisms is available as supplementary material (see Visualization 1).

Cerium is more efficient than lanthanum to mitigate photo-darkening. Indeed, at low concentration, *Ce* and *La* have a reducing rate of $-1.6 dB/m/ppm.at$ and $-0.16 dB/m/ppm.at$, respectively. *Ce* is ten times more efficient than *La* at low concentration. However, the role of *Ce* is more complex to discuss than *La* because it has two valence states (4+ and 3+) and both of them could combine structural and optical effects. The characterization and the control of the redox is a major issue, particularly in glasses. It depends on many factors such as the ion concentration, the overall composition, the temperature at which the glass was melted, the furnace atmosphere (oxidizing or reducing) [29]. Even in oxidizing conditions, the redox of cerium is not clearly established. Previous reports support the predominance of either Ce^{4+} or Ce^{3+} , but their conclusions are highly dependant on fabrication conditions [14, 19, 30]. When cerium is present as Ce^{4+} , it would be efficient to compensate the charge of Al^{IV} species ($\frac{[Al_2O_3]}{[CeO_2]} \leq 4$ and $\frac{[Al_2O_3]}{[Ce_2O_3]} \leq 3$). This could be a first ex-

planation of the highest rate of photodarkening mitigation by *Ce* as the threshold for charge compensation should be around 2000 *ppm.at Ce*. Ce^{4+} has a charge transfer absorption band peaking at 260 nm and Ce^{3+} has a $4f-5d$ transition at 330 nm [30]. therefore both valence states of *Ce* can absorb UV emitted by *Tm* (mitigating the ionization of defects and releasing electrons in the conduction band (Figure 5 and Visualization 1). Ce^{4+} can also trap the electron released in the conduction band, thus reducing the formation of Tm^{2+} and “Defect 2”.

In summary, series of MCVD-made fibers were fabricated containing various concentrations of thulium, lanthanum and cerium. Spectral and time-resolved measurements of photo-induced absorption were performed under high power pumping at 1.07 μm wavelength. PIA spectra are all similar, with a strong visible and a weak near-infrared broad absorption bands. They suggest a charge transfer during photo-darkening, transforming Tm^{3+} into Tm^{2+} . PIA increases with *Tm* concentration. The lanthanum and the cerium co-doping are found to behave as hardeners against photo-darkening. Those effects are tentatively assigned to their structural and optical effects. It is found that cerium is a very good additive for reducing photo-darkening because 95% of this detrimental effect is bleached by adding 1300 *ppm.at* of *Ce*. It is also found that *La* can reduce photo-darkening by 70%. We believe that this quantitative study contributes to the understanding of photo-degradation of Tm-doped fibers under 1.07 μm pumping with the aim of developing of powerful fiber amplifiers at wavelengths shorter than 0.85 μm . First, the 1300-ppm *Ce* sample PIAst is 10 times lower than Tm absorption in the NIR, so amplification would be achievable along the $^1G_4 \rightarrow ^3F_4$ transition at 0.785 μm . Further, increasing of the cerium concentration is possible without loss of glass quality up to 0.55% of non-oxygen elements at least (≥ 10 times more than in our samples) [10]. This would further lower PIAst levels, and hence allow for amplification at shorter wavelengths.

Funding. Universit Nice Sophia Antipolis, Centre National de la Recherche Scientifique, Agence Nationale de la Recherche (ANR-14-CE07-0016-01, Nice-DREAM).

Acknowledgements. We thank S. Trzesien and M. Ude (LPMC, Nice) for the fabrication of the samples, M. Fialin (IPGP Camparis) for EPMA measurements and B. Gay-Para (LPMC, Nice) for the preparation of the animated sequence.

References

- [1] DJ Richardson, J Nilsson, and WA Clarkson. High power fiber lasers: current status and future perspectives [invited]. *J. Opt. Soc. Am. B*, 27(11):B63–B92, 2010.
- [2] B Leconte, B Cadier, H Gilles, S Girard, T Robin, and M Laroche. Extended tunability of Nd-doped fiber lasers operating at 872–936 nm. *Opt. Lett.*, 40(17):4098–4101, 2015.
- [3] Xiushan Zhu and N Peyghambarian. High-power ZBLAN glass fiber lasers: review and prospect. *Adv. Optoelectron.*, 2010, 2010.
- [4] DC Hanna, IM Jauncey, RM Percival, IR Perry, RG Smart, PJ Suni, JE Townsend, and AC Tropper. Continuous-wave oscillation of a monomode thulium-doped fibre laser. *Electron. Lett.*, 24(19):1222–1223, 1988.

- [5] MM Broer, DM Krol, and DJ DiGiovanni. Highly nonlinear near-resonant photodarkening in a thulium-doped aluminosilicate glass fiber. *Opt. Lett.*, 18(10):799–801, 1993.
- [6] Wilfried Blanc, Thomas Lee Sebastian, Bernard Dussardier, Claire Michel, Basile Faure, Michèle Ude, and Gérard Monnom. Thulium environment in a silica doped optical fibre. *J. Non-Cryst. Solids*, 354(2):435–439, 2008.
- [7] Basile Faure, Wilfried Blanc, Bernard Dussardier, and Gérard Monnom. Improvement of the $\text{Tm}^{3+} : ^3\text{H}_4$ level lifetime in silica optical fibers by lowering the local phonon energy. *J. Non-Cryst. Solids*, 353(29):2767–2773, 2007.
- [8] JMF Van Dijk and MFH Schuurmans. On the nonradiative and radiative decay rates and a modified exponential energy gap law for 4f–4f transitions in rare-earth ions. *J. Chem. Phys.*, 78(9):5317–5323, 1983.
- [9] Sylvia Jetschke, Sonja Unger, Anka Schwuchow, Martin Leich, Julia Fiebrandt, Matthias Jäger, and Johannes Kirchhof. Evidence of Tm impact in low-photodarkening Yb-doped fibers. *Opt. Express*, 21(6):7590–7598, 2013.
- [10] M Engholm, P Jelger, F Laurell, and L Norin. Improved photodarkening resistivity in ytterbium-doped fiber lasers by cerium codoping. *Opt. Lett.*, 34(8):1285–1287, 2009.
- [11] Magnus Engholm and Lars Norin. Preventing photodarkening in ytterbium-doped high power fiber lasers; correlation to the UV-transparency of the core glass. *Opt. Express*, 16(2):1260–1268, 2008.
- [12] Doris Litzkendorf, Stephan Grimm, Kay Schuster, Jens Kobelke, Anka Schwuchow, Anne Ludwig, Johannes Kirchhof, Martin Leich, Sylvia Jetschke, and Jan Dellith. Study of lanthanum aluminum silicate glasses for passive and active optical fibers. *IJAGS*, 3(4):321–331, 2012.
- [13] Sylvia Jetschke, Sonja Unger, Ulrich Röpke, and Johannes Kirchhof. Photodarkening in Yb doped fibers: experimental evidence of equilibrium states depending on the pump power. *Opt. Express*, 15(22):14838–14843, 2007.
- [14] S Unger, A Schwuchow, S Jetschke, St Grimm, A Scheffel, and J Kirchhof. Optical properties of cerium-codoped high power laser fibers. *SPIE OPTO*, 8621:16, 2013.
- [15] DS Hamilton, SK Gayen, GJ Pogatshnik, RD Ghen, and WJ Miniscalco. Optical-absorption and photoionization measurements from the excited states of $\text{Ce}^{3+} : \text{Y}_3\text{Al}_5\text{O}_{12}$. *Phys. Rev. B*, 39(13):8807, 1989.
- [16] P Dorenbos. Systematic behaviour in trivalent lanthanide charge transfer energies. *J. Phys. Condens. Matter*, 15(49):8417, 2003.
- [17] A Paul, M Mulholland, and MS Zaman. Ultraviolet absorption of cerium (III) and cerium (IV) in some simple glasses. *J. Mater. Sci.*, 11(11):2082–2086, 1976.
- [18] M Raukas, SA Basun, W Van Schaik, WM Yen, and U Happek. Luminescence efficiency of cerium doped insulators: The role of electron transfer processes. *Appl. Phys. Lett.*, 69(22):3300–3302, 1996.
- [19] WD Johnston. Oxidation-reduction equilibria in molten $\text{Na}_2\text{O} \cdot 2\text{SiO}_2$ glass. *J. Am. Ceram. Soc.*, 48(4):184–190, 1965.
- [20] Yasmine Mebrouk, Franck Mady, Mourad Benabdesselam, Jean-Bernard Duchez, and Wilfried Blanc. Experimental evidence of Er^{3+} ion reduction in the radiation-induced degradation of erbium-doped silica fibers. *Opt. Lett.*, 39(21):6154–6157, 2014.
- [21] Zoltan J Kiss. Energy levels of divalent thulium in CaF_2 . *Phys. Rev.*, 127(3):718, 1962.
- [22] Andre Monteil, Stéphane Chaussement, G Alombert-Goget, N Gaumer, J Obriot, SJL Ribeiro, Younes Messaddeq, A Chiasera, and M Ferrari. Clustering of rare earth in glasses, aluminum effect: experiments and modeling. *J. Non-Cryst. Solids*, 348:44–50, 2004.
- [23] David A Simpson, Gregory W Baxter, Stephen F Collins, WEK Gibbs, Wilfried Blanc, Bernard Dussardier, and Gérard Monnom. Energy transfer up-conversion in Tm^{3+} -doped silica fiber. *J. Non-Cryst. Solids*, 352(2):136–141, 2006.
- [24] R Paschotta, PR Barber, AC Tropper, and DC Hanna. Characterization and modeling of thulium: ZBLAN blue upconversion fiber lasers. *J. Opt. Soc. Am. B*, 14(5):1213–1218, 1997.
- [25] Linards Skuja. Optically active oxygen-deficiency-related centers in amorphous silicon dioxide. *J. Non-Cryst. Solids*, 239(1):16–48, 1998.
- [26] P Florian, N Sadiki, D Massiot, and JP Coutures. ^{27}Al NMR study of the structure of lanthanum- and yttrium-based aluminosilicate glasses and melts. *J. Phys. Chem. B*, 111(33):9747–9757, 2007.
- [27] Jacob L Philipsen, Jes Broeng, A Bjarklev, Sten Helmfrid, Dan Bremberg, B Jaskorzynska, and B Palsdonir. Observation of strongly nonquadratic homogeneous upconversion in Er^{3+} -doped silica fibers and reevaluation of the degree of clustering. *IEEE J. Quant. Electron.*, 35(11):1741–1749, 1999.
- [28] Stavros G Demos, Paul R Ehrmann, S Roger Qiu, Kathleen I Schaffers, and Tayyab I Suratwala. Dynamics of defects in Ce^{3+} doped silica affecting its performance as protective filter in ultraviolet high-power lasers. *Opt. Express*, 22(23):28798–28809, 2014.
- [29] NE Densem and WES Turner. The equilibrium between ferrous and ferric oxides in glasses. *JSGT*, 22:372–89, 1938.
- [30] M Fasoli, A Vedda, A Lauria, F Moretti, E Rizzelli, N Chiodini, F Meinardi, and M Nikl. Effect of reducing sintering atmosphere on Ce-doped sol-gel silica glasses. *J. Non-Cryst. Solids*, 355(18):1140–1144, 2009.